Journal of Nuclear Materials 376 (2008) 169–173

Contents lists available at ScienceDirect

Journal of Nuclear Materials

journal homepage: www.elsevier.com/locate/jnucmat

Analyzing the effect of displacement rate on radiation-induced segregation in 304 and 316 stainless steels by examining irradiated EBR-II components and samples irradiated with protons

T.R. Allen [a,*], J.I. Cole [b], E.A. Kenik [c], G.S. Was [d]

[a] Department of Engineering Physics, University of Wisconsin-Madison, 1500 Engineering Drive, Madison, WI 53706, USA
[b] Idaho National Laboratory, PO Box 2528, Idaho Falls, ID, USA
[c] Oak Ridge National Laboratory, PO Box 2008, Oak Ridge, TN 37831-6064, USA
[d] University of Michigan, 2355 Bonisteel Boulevard, Ann Arbor, MI 48109, USA

ARTICLE INFO

Article history:
Received 3 January 2007
Accepted 2 January 2008

PACS:
61.80.Jh
61.72.Mm
61.82.Bg

ABSTRACT

Recent studies have indicated that, at temperatures relevant to fast reactors and light water reactors, void swelling in austenitic alloys progresses more rapidly when the radiation dose rate is lower. A similar dependency between radiation-induced segregation (RIS) and dose rate is theoretically predicted for pure materials and might also be true in complex engineering alloys. Radiation-induced segregation was measured on 304 and 316 stainless steel, irradiated in the EBR-II reactor at temperatures near 375 °C, to determine if the segregation is a strong function of damage rate. The data taken from samples irradiated in EBR-II is also compared to RIS data generated using proton radiation. Although the operational histories of the reactor irradiated samples are complex, making definitive conclusions difficult, the preponderance of the evidence indicates that radiation-induced segregation in 304 and 316 stainless steels is greater at lower displacement rate.

1. Introduction

Radiation-induced segregation is a non-equilibrium process that occurs at grain boundaries and other defect sinks such as dislocation loops and voids during irradiation of an alloy at high temperature (30–50% of the melting temperature) [1]. In irradiated iron–chromium–nickel alloys, nickel enriches and chromium depletes at defect sinks. Iron either enriches or depletes depending on the bulk alloy composition.

Wolfer et al. theoretically predicted that segregation will change the bias of defect sinks for point defects [2–4]. Because of the possible link between RIS and microstructural development, and the growing body of evidence on a dose rate dependence on swelling, the relationship between dose rate and RIS is important. A series of 304 and 316 stainless steel components were retrieved from the EBR-II reactor following irradiation. Samples were taken from reactor components removed from the reflector region of EBR-II following the final shutdown. Since they are real reactor components and not test specimens, they were irradiated at a variety of temperatures and dose rates. Fig. 1 shows the dose rate at core centerline as a function of radial position. In the reflector region (rows 7 and higher), the dose rate changes considerably as a function of position. RIS was measured at grain boundaries on these samples to investigate the effect of dose rate on RIS. These measurements from EBR-II materials were also compared to RIS measurements from similar alloys irradiated with high-energy protons.

2. Experiment

Samples of 316 stainless steel were taken from a reflector subassembly irradiated in row 8 of EBR-II. These subassemblies were 20% cold-worked 316. Specimens were taken at various axial locations in the reflector subassembly so that irradiation conditions of 1, 20, and 30 dpa were analyzed. As all of the samples were taken from different axial positions of the same subassembly, each had a different dose rate and temperature. The temperature differences were small (<6 °C). The dose rate variation corresponded with the dose variation (a ratio of 1:20:30 dpa/s). Bulk composition of the 316 was determined from available archive material.

Samples of 304 stainless steel were taken from row 10, 14, and 16 reflector subassemblies and from surveillance (SURV) samples irradiated in row 12. The 304 samples were not all from the same lot of steel. Bulk compositions for all of the samples are listed in Table 1. Since archive material was not available for the samples from row 14, composition was determined from samples taken from an irradiated 304 hex duct using inductively coupled

* Corresponding author. Tel.: +1 608 265 4083; fax: +1 608 263 7451.
E-mail address: allen@engr.wisc.edu (T.R. Allen).

0022-3115/$ - see front matter © 2008 Elsevier B.V. All rights reserved.
doi:10.1016/j.jnucmat.2008.01.025

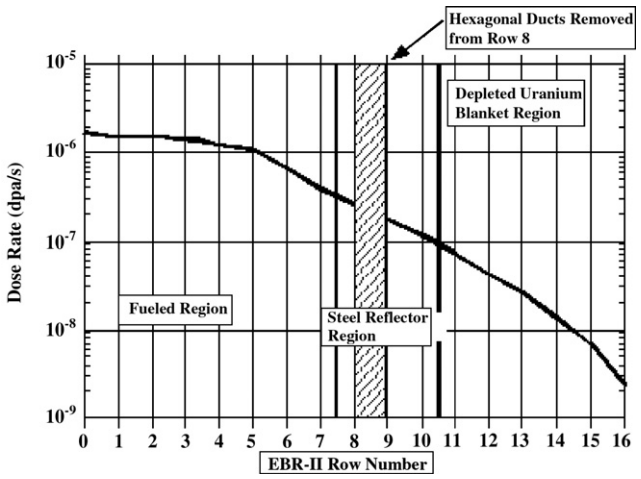

Fig. 1. Dose rate as a function of radial core position in EBR-II at core centerline.

Table 1
Bulk compositions for microchemistry samples

Element	Row 8, 316 (at.%)	Row 10, 16 304 (at.%)	Row 12, 304 (at.%)	Row 14, 304 (at.%)
Cr	18.4	19.6	19.4	19.6
Ni	12.5	8.5	9.4	9.1
Fe	65.6	69.8	68.4	69.0
Mo	1.9	<0.02	0.12	0.07
Mn	0.8	0.82	0.90	1.01
C	0.4	0.4	0.4	0.5
Si	0.4	0.92	1.3	0.76

plasma-atomic emission spectroscopy (ICP-AES) for major elements and a LECO IR-412 Carbon Determinator for carbon.

The sample irradiation histories for all of the samples are listed in Table 2. All doses and temperatures are calculated and represent averages over the lifetime of the sample. Two samples were taken from reflectors that were moved once during their lifetime. The 'Row 14 sample' spent approximately 1.5% of its time in core in row 8. During the time in row 8 (position 8F4), the temperature of the samples from the row 14 subassembly was 390 °C. The 'Row 16 sample' spent approximately 36% of its time in core in row 8 (position 8A3).

Grain boundary compositions were measured using scanning transmission electron microscopy with energy dispersive X-ray spectrometry (STEM/EDS). The STEM/EDS was performed at an accelerating voltage of 200 kV on a Philips CM200 equipped with a field emission gun source at Oak Ridge National Laboratory. STEM/EDS measurements were performed at the grain boundary and at increments of 1.0 nm away from the boundary to give compositional profiles. The incident probe diameter was approximately 1.4 nm (full width, tenth maximum). The sample was tilted towards the X-ray detector and each grain boundary analyzed was aligned such that the boundary was 'edge-on' (parallel to the electron beam). This alignment minimizes the effect of geometric broadening of the measured profiles by an inclined boundary. Although in all of the irradiated samples, portions of the grain boundaries contained precipitates, limited areas free of precipitation were found and grain boundaries were profiled in these precipitate free areas. The number of boundaries for any specific irradiation condition ranged from as small as two to as high as fifteen for EBR-II materials. Proton-irradiated samples provided as many as 50 boundaries for analysis. In all figures and tables, the average segregation and associated uncertainty are provided.

3. Results and discussion

The segregation data taken from samples of 304 stainless steel will be presented first and then a comparison of segregation in 304 and 316 will follow. The materials examined in this study were taken from irradiated core components and were not placed in the reactor as an experiment designed to elucidate dose rate effects on RIS. In each case, factors such as varying alloy composition within a material class or operational history complicate the analysis. Nonetheless, the breadth of the measurements, along with references to recently published data, indicate strongly that decreasing the dose rate leads to greater radiation-induced segregation.

3.1. Segregation in 304 stainless steel

Since archive material was available from the steel used to fabricate subassemblies in rows 10 and 16, grain boundary composition measurements were taken in an unirradiated sample of the row 10/16 steel. A slight chromium enrichment and iron depletion (~2.5 at.% for each) exists. No indication of grain boundary precipitates exists prior to radiation. No archive material was available for the row 12 and row 14 samples so no unirradiated measurements are possible.

Chromium depletion and nickel enrichment, measured in components made of 304 stainless steel irradiated in rows 10, 12, and 14 of EBR-II, are presented in Fig. 2. The larger the row number, the lower the dose rate. All three measurements were taken on samples irradiated with average temperatures between 375 and 380 °C. The total dose on the row 12 sample is about twice that on the samples from row 10 and 14. The row 14 sample, which was irradiated at the lowest average displacement rate, has greater chromium depletion and nickel enrichment than either the row 10 or row 12 samples, even at half the dose of the row 12 sample. The comparison is complicated by the fact that the row 14 sample received 25% of its total dose in row 8, a higher dose rate position,

Table 2
TEM Sample History

Sample	Material	Reactor grid position	Time in grid position (MWD[a])	Dose rate (dpa/s) in grid position	Average dose rate (dpa/s)	Dose (dpa) in grid position	Total dose (dpa)	Average temperature (°C)
Row 8	316	8D6	122 000	7.6×10^{-8}	7.6×10^{-8}	1.0	1.0	373
Row 8	316	8D6	122 000	1.2×10^{-7}	1.2×10^{-7}	20.0	20.0	375
Row 8	316	8D6	122 000	1.8×10^{-7}	1.8×10^{-7}	30.0	30.0	379
Row 10	304	10C2	187 505	4.7×10^{-8}	4.7×10^{-8}	12.2	12.2	378
Row 12	304	12E8	215 110	6.6×10^{-8}	6.6×10^{-8}	19.6	19.6	389
Row 14	304	8F4	5951	2.9×10^{-7}	2.0×10^{-8}	2.4	10	379
		14E10	348 584	1.5×10^{-8}		7.6		
Row 16	304	8A3	60 165	1.2×10^{-7}	4.6×10^{-8}	10.3	10.6	375
		16B9	107 495	2.0×10^{-9}		0.3		

[a] MWD: Megawatt-Days.

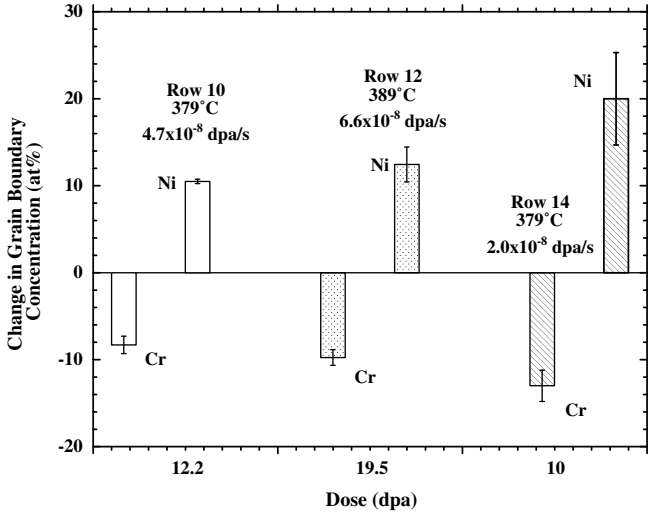

Fig. 2. Grain boundary chromium depletion and nickel enrichment in 304 stainless steel irradiated in EBR-II. Row 10 and row 14 data come from the average of two measurements. Row 12 is the average of 3 measurements.

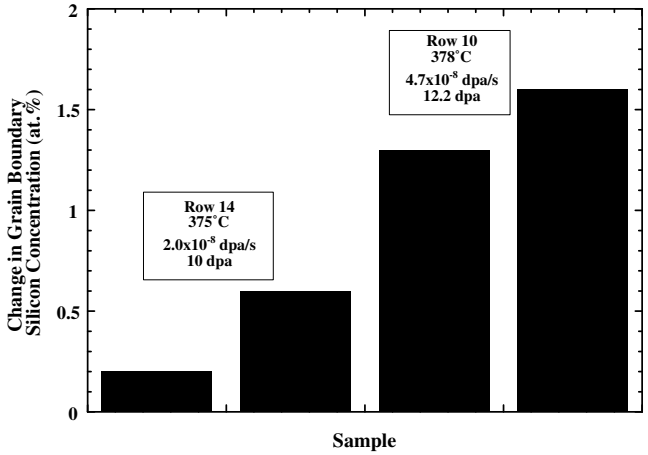

Fig. 3. Grain boundary silicon segregation. Two segregation measurements are presented from each radiation condition.

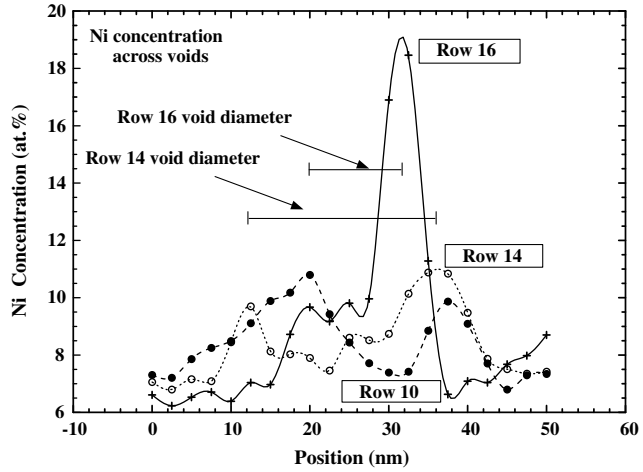

Fig. 4. Nickel segregation profile across voids in three samples irradiated at similar temperature (~375–380 °C) and dose (~10–12 dpa), but with varying dose rate.

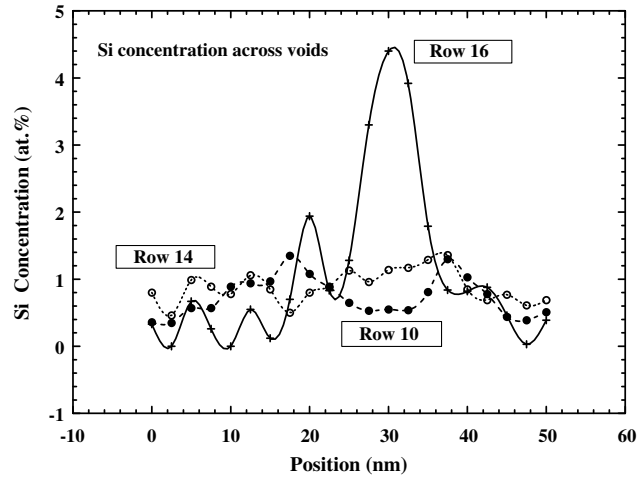

Fig. 5. Silicon segregation profile across voids in three samples irradiated at similar temperature (~375–380 °C) and dose (~10–12 dpa), but with varying dose rate.

before being moved to row 14. Calculations indicate that the segregation in the row 14 position should have reached a new steady-state at the lower dose rate during the last 7.6 dpa of irradiation (occurring over approximately 15 years) [5]. The data in Fig. 2 suggest that greater segregation of chromium and nickel is possible at lower dose rate, although the conclusion is complicated by the operational history of the samples.

The row 14 subassembly has significantly greater bulk molybdenum than the row 10 subassembly. Segregation measurements in samples from Magnox reactor control rods (a 4 wt% boron steel) irradiated at temperatures from 290 to 330 °C to doses from 0.04 to 0.35 dpa, indicated that increasing bulk Mo content reduced the Cr depletion [6]. In the EBR-II samples, greater grain boundary chromium depletion occurs in the sample with greater bulk molybdenum concentration, contrary to the Magnox measurements. Since the differences in chromium depletion in the EBR-II materials do not correlate with differences in bulk Mo composition, the differences may be caused by differences in irradiation history.

The row 10 subassembly does also have a slightly larger bulk silicon concentration than the row 14 subassembly. Carter et al. have shown that for ultra high purity 304 L alloys, increasing the bulk silicon concentration by a factor of 10 increases the chromium depletion and nickel enrichment at grain boundaries [7]. Therefore, the difference in bulk silicon is an unlikely explanation for the difference in chromium and nickel segregation seen between EBR-II samples.

Grain boundary silicon concentration was also measured in the row 10 and row 14 samples and is presented in Fig. 3. The silicon segregation differs from the bulk chromium and nickel segregation in that greater Si enrichment occurs at higher dose rate. Since the silicon enrichment is greater in the high dose rate sample (which had less major element segregation), the silicon enrichment is not coupled to the major element segregation. For example, if Ni and Si were bound together, the enrichment of Ni should lead to an enrichment of Si. This coupling (or binding) is not seen and may indicate the driving mechanism for segregation differs.

Composition profiles were taken across voids in the samples from rows 10, 14, and 16. Figs. 4 and 5 plot the typical nickel and silicon concentration across voids from all three samples. In the row 16 sample, a large fraction of the voids were paired with silicon-rich precipitates, but the profiles in Figs. 4 and 5 were for a void that appeared precipitate free. The row 10 and 14 samples have similar segregation profiles for nickel and silicon, while in the row 16 sample, the nickel and silicon enrichment are much more pronounced on one side of the void. In all three samples, the nickel segregation is greater on one side of the void. Note that

the void size is different for each profile and a comparison of composition at the same position on the graph has no significance. The void edges can be located by the maxima in the nickel composition.

The segregation from the EBR-II samples can be compared to segregation in other 304 stainless steel samples irradiated at similar temperature. Dumbill measured segregation in an Fe–18Cr–15Ni alloy irradiated with neutrons at 400 °C to 12.7 dpa in EBR-II [8]. A dose rate was not reported, but a typical experimental location in EBR-II had dose rates on the order of 10^{-6} dpa/s. In these samples, the grain boundary nickel concentration was 8 at.% greater than the bulk and the grain boundary chromium concentration was 7 at.% less than the bulk (see Fig. 6). Williams et al. [9] measured the segregation in 304 stainless steel taken from a PWR control rod thimble plug irradiated to fluences of 5×10^{21} n/cm^2 ($E > 0.1$ MeV) (an approximate dose of 7 dpa). The dose rate and temperature were not reported. Unirradiated boundaries showed a chromium enrichment and iron depletion (about 7 at.%). In the irradiated samples, the grain boundary chromium concentration was 2 at.% less than bulk and the grain boundary nickel was approximately 8 at.% greater than the bulk.

The EBR-II hex duct materials had greater major element segregation than seen in both of the referenced studies. In the work by Dumbill, the Fe–18Cr–15Ni alloy has a greater bulk nickel concentration and was irradiated at a higher temperature and therefore would be expected to exhibit greater nickel enrichment [10] for similar irradiation conditions. The greater segregation in the EBR-II materials is likely attributable to a dose rate difference. The greater chromium enrichment in the unirradiated material of the Williams study may explain the smaller chromium depletion in the irradiated materials, but without temperature and dose rate information, no further comparison to the EBR-II materials can be made.

The segregation of 304 stainless steel irradiated with protons at 360 °C, 7×10^{-6} dpa/s, to a final dose of 5.5 dpa [11] is compared to the segregation measured in the row 10 304 subassembly in Table 3. If efficiency for producing freely migrating defects (FMD) is about 0.2 for proton irradiations and 0.05 for neutron irradiations [12], then the EBR-II and proton-irradiated samples were irradiated to roughly the same equivalent dose (0.6 dpa for the EBR-II steel and 1.1 dpa for the proton-irradiated steel) and at similar temperatures. The segregation is larger in the samples from EBR-II (even at slightly lower equivalent dose) that were irradiated at a much lower dose rate.

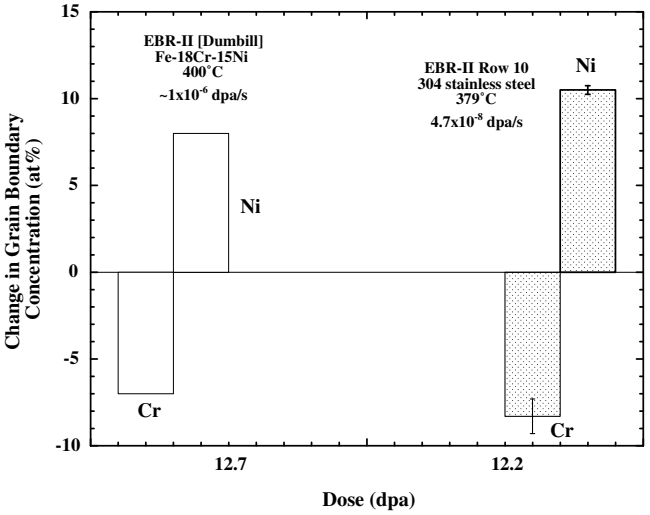

Fig. 6. Comparison of segregation measured on samples irradiated in the high flux and low flux regions of EBR-II. Dumbill data is a single measurement. EBR-II data is the average of two measurements.

Table 3
Comparison of grain boundary compositions between proton and neutron irradiated 304 stainless steel (change between bulk and boundary in at.%)

Element	Proton irradiation 360 °C, 5.5 dpa	EBR-II (row 10 sample) 378 °C, 12.2 dpa
Cr	−6.1	−8.3
Ni	+8.2	+10.5
Fe	−1.5	−3.6

Little other data exists on the dose rate effect on RIS, but the data that exists supports the dose rate effect seen in the EBR-II studies. Chatani et al. studied the effect of dose rate on segregation by comparing 304 stainless irradiated at high flux in a fast reactor with 304 from the same lot of material irradiated at low flux in a pressurized water reactor (PWR) [13]. For nearly constant fluence, the nickel enrichment was greater in the sample irradiated in the low flux PWR.

3.2. Comparing segregation in 304 and 316 stainless steel

Measurements have indicated that for identical low dose irradiation conditions, the segregation is larger in alloys with larger bulk nickel concentration [11,14]. This is demonstrated in Fig. 7 using segregation measurements from 304, 316, Fe–18Cr–8Ni (corresponding to 304), and Fe–16Cr–13Ni (corresponding to 316) that were irradiated with 3.2 MeV protons at 360 and 400 °C to 1.0 dpa. For two different temperatures, on both steels and model alloys, the segregation is greater in alloys with larger bulk nickel. For alloys with lower bulk nickel concentration, the segregation profiles develop more slowly and at higher doses, the segregation is greater [10]. This is shown in Table 4 that compares proton-irradiated data at 360 °C to 1.0 and 5.5 dpa. At higher dose, the segregation in 304 becomes slightly (roughly 50%) greater than in 316.

The chromium depletion and nickel enrichment of 304 and 316 is shown in Fig. 8 for samples irradiated in EBR-II to ~20 dpa at much different dose rates. The 316 was irradiated at about twice the dose rate of the 304. The 304 stainless steel was mill annealed and the 316 stainless steel was 20% cold-worked prior to irradiation so both materials had significant dislocation densities prior to irradiation (although the mill annealed 304 will have less

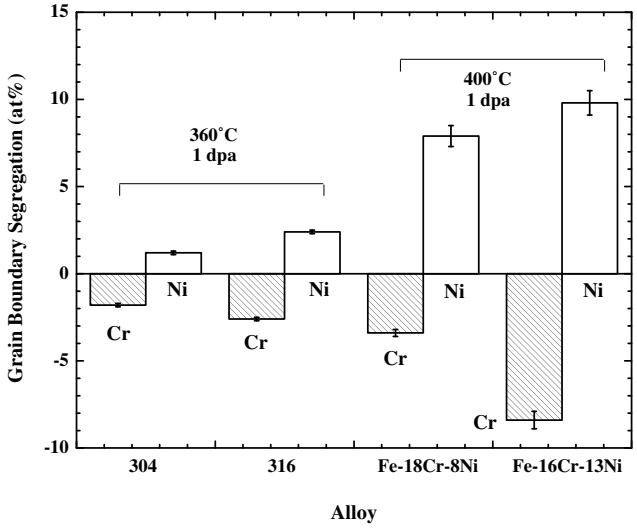

Fig. 7. Comparison of segregation between 304 and 316 stainless steel, as well as model alloys based on 304 and 316, irradiated with 3.2 MeV protons. Uncertainties are the standard deviation of the mean. Each bar is based on between 18 and 50 measurements.

Table 4
Comparison of grain boundary compositions between proton-irradiated 304 and 316 stainless steels (each reported value has an uncertainty of ±0.2)

Element	Proton irradiation 360 °C, 1.0 dpa		Proton irradiation 360 °C, 5.5 dpa	
	304 SS	316 SS	304 SS	316 SS
Cr	−1.8	−2.6	−6.1	−4.3
Ni	+1.2	+2.6	+8.2	+6.4

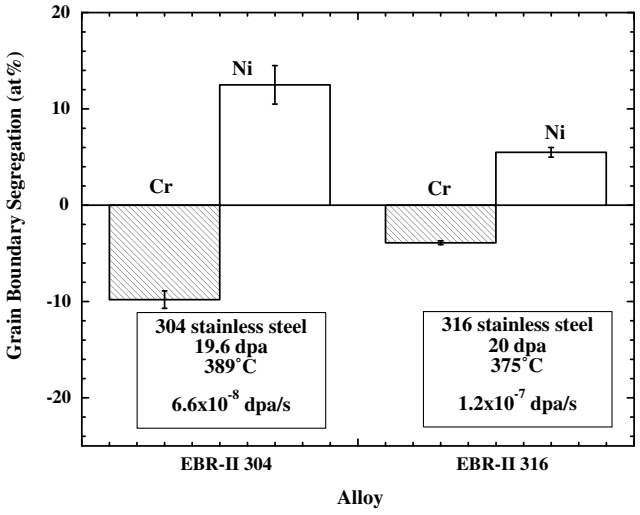

Fig. 8. Comparison of RIS in 304 and 316 stainless steel irradiated to ~20 dpa. Plotted average based on three grain boundary measurements for the 304 sample and fifteen measurements for the 316 sample.

dislocations than the 20% cold-worked state, a significant dislocation density remains after the mill annealing). The segregation is much larger in 304 than in 316 (a factor of 2 for Ni and a factor of 3 for Cr). The significantly greater segregation in 304 is likely the result of difference in dose rate since under identical conditions, 316 would have segregation closer to 304 as evidenced by the 5.5 dpa proton irradiation data from Table 4.

4. Conclusions

To understand the effect of displacement rate on radiation-induced segregation, measurements were taken on samples of 304 and 316 stainless steel irradiated at temperatures near 375 °C in the EBR-II reactor and compared with much higher dose rate data from proton irradiation. The materials examined in this study were taken from irradiated core components and were not placed in the reactor as an experiment designed to elucidate dose rate effects on RIS. In each case, factors such as varying alloy composition within a material class or operational history complicate the analysis. Nonetheless, the breadth of the measurements, along with references to recently published data, indicate strongly that decreasing the dose rate leads to greater radiation-induced segregation. Although the operational history of the reactor components from which samples were taken was complex and complicates analysis, the evidence supports greater chromium depletion and nickel enrichment for samples irradiated at lower displacement rate. The limited data on silicon enrichment indicates the opposite trend with silicon enrichment being greater at higher dose rate.

Acknowledgements

Research at the Oak Ridge National Laboratory SHaRE User Facility was sponsored by the Division of Materials Sciences and Engineering, US Department of Energy under contract DE-AC05-00OR22725 with UT-Battelle, LLC.

References

[1] P.R. Okamoto, L.E. Rehn, J. Nucl. Mater. 83 (1979) 2.
[2] A. Si-Ahmed, W.G. Wolfer, in: H.R. Brager, J.S. Perrin (Eds.), Effects of Radiation on Materials: Eleventh Conference, ASTM STP 782, American Society for Testing and Materials, 1982, p. 1008.
[3] W.G. Wolfer, L.K. Mansur, J. Nucl. Mater. 91 (1980) 265.
[4] J.J. Sniegowski, W.G. Wolfer, in: Proceedings of Topical Conference on Ferritic Alloys for Use in Nuclear Energy Technologies, Snowbird, Utah, 19–23 June 1983.
[5] G.S. Was, T. Allen, J. Nucl. Mater. 205 (1993) 332.
[6] P. Spellward, J. Walmsley, R. Scowen, N. Partridge, J. Stump, R. Corcoran, T. Gilmour, V. Callen, in: Proceedings of Eighth International Symposium on Environmental Degradation of Materials in Nuclear Power Systems – Water Reactors, Amelia Island, Fl, August 1997, American Nuclear Society, LaGrange Park, IL, 1997, p. 734.
[7] R.D. Carter, D.L. Damcott, M. Atzmon, G.S. Was, E.A. Kenik, J. Nucl. Mater. 205 (1993) 361.
[8] S. Dumbill, T.M. Williams, in: Proceedings of the Conference on Materials for Nuclear Reactor Core Applications, vol. 1, BNES, London 1987, p. 119.
[9] J.F. Williams, P. Spellward, J. Walmsley, T.R. Mager, M. Koyama, H. Mimaki, I. Suzuki, Proceedings of the Eighth International Symposium on Environmental Degradation of Materials in Nuclear Power Systems – Water Reactors, Amelia Island, Fl, August 1997, American Nuclear Society, LaGrange Park, IL, 1997, p. 725.
[10] T.R. Allen, J.T. Busby, G.S. Was, E.A. Kenik, J. Nucl. Mater. 255 (1998) 44.
[11] G.S. Was, T.R. Allen, J.T. Busby, J. Gan, D. Damcott, D. Carter, M. Atzmon, E.A. Kenik, J. Nucl. Mater. 270 (1999) 96.
[12] S.J. Zinkle, B.N. Singh, J. Nucl. Mater. 199 (1993) 173.
[13] K. Chatani, Y. Kitsunai, M. Kodama, S. Suzuki, Y. Tanaka, S. Ooki, S. Tanaka, T. Nakamura, in: Todd R. Allen, Peter J. King, Lawrence Nelson (Eds.), 12th Environmental Degradation Conference of Materials in Nuclear Power Systems – Water Reactors, TMS, 2006, p. 349.
[14] T.R. Allen, J.I. Cole, N.L. Dietz, Y. Wang, G.S. Was, E.A. Kenik, in: Proceedings of the MRS Fall Meeting: Microstructure Processes in Irradiated Materials-2000, vol. 650, Materials Research Society, Warrendale, PA, 2000, p. R3.12.